

# Contact-Damage Resistance of Partially Leached Glasses

P. CHANTIKUL, D. B. MARSHALL, and B. R. LAWN\*

Department of Applied Physics, School of Physics, The University of New South Wales, New South Wales 2033, Australia

M. G. DREXHAGE\*

Deputy for Electronic Technology, Rome Air Development Center, Hanscom Air Force Base, Massachusetts 01731

**Strength degradation characteristics of partially leached glass rods damaged in sharp contact are investigated. Residual compressive stresses in the outer layer (clad) of the treated rods inhibit the growth of surface cracks toward the inner region (core). The strength of rods indented quasi-statically with a Vickers diamond pyramid shows functional dependences on contact load and clad stress in good agreement with predictions based on indentation fracture theory. The analysis identifies the degree of residual compression as the key parameter in the strengthening effect; however, in designing for high-performance applications it may be necessary to optimize material properties (e.g. toughness, elastic moduli) and dimensions of the clad/core composite. Partial leaching, with its potential for developing high, uniform stresses over the clad thickness, may be advocated as a most useful means of obtaining high resistance to adverse contact conditions.**

## I. Introduction

**W**ITH the increasing call for glasses of high mechanical integrity, particularly in the optical fiber industry, there is special

interest in the development of surface strengthening techniques. In certain circumstances it may be possible to achieve strengths close to the intrinsic limit by suitably protecting the pristine surfaces from potentially hostile surroundings. However, in most applications, the general susceptibility of brittle surfaces to the incidence of mechanical handling damage renders this approach ineffective; strengthening then becomes a matter of combating the growth of flaws. By far the most practical means of achieving this end is to introduce a state of residual compression into the surfaces.<sup>1</sup> Secondary benefits, such as improved chemical durability and thermal shock resistance, make surface compression an attractive tool in designing against failure of glass components.

The best established way of putting a glass surface into residual compression is by thermal tempering. However, this method does not improve the strength of as-received surfaces by much more than a factor of two. Ion-exchange techniques are capable of generating considerably higher surface compressions, but over a much thinner surface layer. Consequently, neither of these two widely used

Received January 15, 1979.

Supported by the Australian Research Grants Committee.

\*Member, the American Ceramic Society.

techniques is entirely satisfactory in providing high resistance to contact damage.<sup>2</sup> The ideal combination of high stress intensity and large spatial extent in the surface compression layer is not easily produced in brittle materials.

One procedure which shows considerable promise in this particular aspect of glass strengthening is that of partial leaching.<sup>3,4</sup> Basically, the procedure involves the following steps: an appropriate alkali borosilicate glass is heat-treated to induce an interconnected two-phase microstructure, one phase being high in silica content and the other containing the borates and alkalis; the latter phase is then leached out to a desired depth below the surface, leaving a porous outer layer (clad) surrounding a solid inner region (core); the glass structure is then heated to consolidate the porous matrix. The result of this treatment is a well-defined step profile in composition across the section of the glass. Differential thermal properties between clad and core accordingly lead to the generation of a corresponding residual stress profile. Although the trade-off between high stress and layer depth (i.e. clad thickness) is not eliminated by this method, the spatial constancy of the pertinent compressive stresses beneath the surface are especially conducive to improved fracture resistance.

In this work the strength characteristics of partially leached glasses are examined, with particular reference to degradation resistance in prospective contact-damage situations. An indentation/strength test procedure<sup>5</sup> is used to obtain data in a controlled manner, with the specific aim of providing information on intrinsic strengthening mechanisms; a major advantage of this procedure is the avoidance of any need for knowledge of preexisting flaw distributions. The results presented here provide useful design parameters for high-performance engineering applications.

## II. Experimental Procedure

### (1) Preparation and Properties of Partially Leached Glass Specimens

A systematic study of the partial-leaching process has shown ensuing properties to depend sensitively on preparation history.<sup>3</sup> For this reason essential details of the glass treatment need to be specified in the description below.

Glass rods (100 mm long by 6 to 8 mm thick) were produced from the following melt composition (in mol%):  $\text{SiO}_2$  62.3,  $\text{B}_2\text{O}_3$  32.3,  $\text{Na}_2\text{O}$  1.80, and  $\text{K}_2\text{O}$  3.57. These rods were heat-treated at 515°C for 120 h to develop the requisite two-phase microstructure, then cooled at 2°C/min to below 350°C; final cooling to room temperature was carried out by exposure to laboratory atmosphere. An etch treatment for 5 min in dilute HF (2.5 vol%) was used to remove spurious surface contamination at this stage. Leaching of the borate and alkali phase was then conducted in a 3*N* solution of HCl at 95°C, leaving a porous silica-rich clad about a solid two-phase core; the clad thickness could be controlled simply by varying the leaching time. To halt the leaching process and to displace excess acid the rods were soaked for 2 to 24 h in methanol. This was followed by heating to 840°C, over a period of 6 h, during which time all traces of solvent were driven off. The specimens were held at this temperature for 15 to 30 min to allow the porous layer to sinter; consolidation was deemed complete when the rods appeared completely clear. Finally, the heated rods were quenched to room temperature, either rapidly in water or relatively slowly in air.

The treated rods were subsequently examined by photoelastic means to determine the residual stress state. Particular attention was devoted to the axial stress  $\sigma_z$  (Fig. 1), this being the component of direct relevance to the commonly observed mode of rod failure, namely flexure. Within an experimental scatter of  $\approx 5\%$ , the birefringence observations confirmed the constancy of the residual compression  $\sigma_R$  through the clad thickness, i.e.  $\sigma_z = -\sigma_R = \text{constant}$  for all  $a < r \leq b$ , where  $a$  and  $b$  are the radii of core and clad, respectively. Absolute determinations of  $\sigma_R$  from the birefringence were made using a stress optical coefficient ( $4.00 \pm 0.08$ )  $\text{TPa}^{-1}$  calibrated from a control test on pure clad material\*: In this test a disk cut from a rod of fully leached glass was

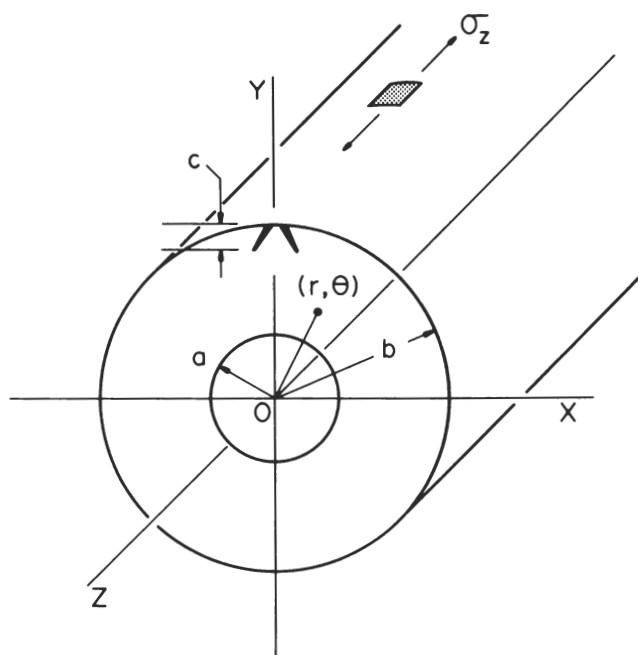


Fig. 1. Coordinate system for analyzing residual-stress distribution and indentation fracture mechanics in partially leached glass rods. Section plane *OXY* shows radii  $a$  and  $b$  of core and clad composite, and depth  $c$  of cone-like indentation crack. Axial stress  $\sigma_z$  is principal strength-determining component of residual field.

loaded uniaxially along its diameter and the resultant birefringence along its axis was matched to the calculated stress components at the center.<sup>6</sup>

For any prescribed set of process variables the stress  $\sigma_R$  is uniquely determined by the ratio  $a/b$ ; generally,  $\sigma_R$  increases with this ratio. The observed form of this stress dependency has been shown<sup>3,4</sup> to be reasonably consistent with the Krohn-Cooper thermal stress model for coaxial glass cylinders in instantaneous cooling,<sup>7</sup> according to which the residual stresses are generated primarily by differences in thermal expansion coefficient and glass transition temperature between clad and core. However, the results in Fig. 2 for partially leached rods subjected to water- and air-quench treatments show that other variables must play at least a secondary role. The lower stresses developed in air quenching are attributed to stress-relaxation effects during the relatively slow cooling period.<sup>3</sup>

### (2) Indentation/Strength Tests

The partially leached glass rods were subjected to controlled surface damage treatments to introduce well-defined starting flaws for strength testing. In most cases this was done using a Vickers diamond pyramid indenter at some preselected load. The contact site was positioned midway along the rod, with the indentation diagonals aligned parallel and perpendicular to the cylinder axis. The fracture pattern produced was somewhat atypical of that generally associated with sharp indenters, in that the dominant penetrative crack resembled more a "cone" than a "median" crack.<sup>8</sup> Such "anomalous" behavior occurs in all glasses of high silica content, apparently as a direct manifestation of a densification mode of irreversible deformation beneath the indenter tip.<sup>9</sup> Figure 3 illustrates the crack geometry in profile.

A few rods were given an alternative, abrasion treatment in place of the indentation. A barrel mill containing 30-mesh SiC grit was used for this purpose.

Strength testing of the rods was carried out in 4-point bending, with the contact site on indented specimens carefully oriented for maximum tensile stress. The failure stress was evaluated from the formula for rod flexure,

$$\sigma = 2kQ(l_o - l_i)/\pi b^3 \quad (1)$$

where  $Q$  is the breaking load,  $l_o$  and  $l_i$  are the outer and inner

\*This value differs from the 3.45 usually quoted for Vycor glass, the composition of which the present clad material is expected to resemble (Ref. 3).

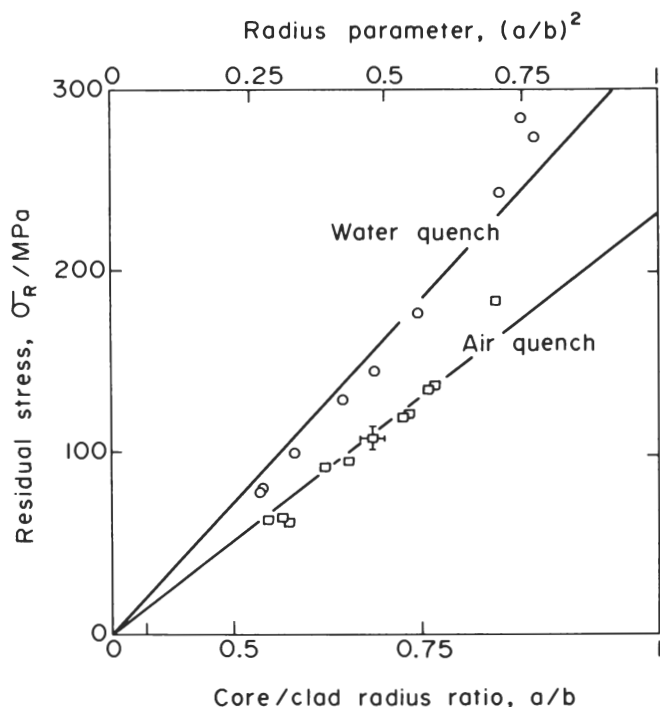


Fig. 2. Plot of  $\sigma_R$  vs  $(a/b)$  for rods subjected to water and air quenching in partial-leaching treatment. Point with error bar represents mean and standard deviation of 15 specimens. Smooth lines are data fits, in approximate accordance with Krohn-Cooper model (Ref. 7).

half-spans,  $b$  is the rod radius, and  $k$  is a dimensionless constant, equal to unity for homogeneous rods. It was necessary in the present experiments to give special attention to the fact that the rods are *not* homogeneous in composition across their section. Differences in Young's moduli  $E_a$  and  $E_b$  of core and clad materials, respectively, must correspondingly modify the stress distribution across the rod: detailed analysis (Appendix A) shows that this effect can be accommodated in Eq. (1) by writing

$$k = 1/[1 + (E_a/E_b - 1)(a/b)^4] \quad (2)$$

Independent measurements and calculations of the two moduli for the glass rods used here (Appendix B) gave  $E_a = 46.5$  GPa and  $E_b = 63.0$  GPa. Thus in the limit of infinitesimally thin clad, i.e.  $a \rightarrow b$ , Eq. (2) yields  $k \rightarrow E_b/E_a = 1.35$ , so the conventional strength formula with  $k = 1$  may be modified by anything up to 35%.

All indentation/strength tests were run with a drop of paraffin oil placed on the prospective contact site, to minimize moisture-assisted kinetic effects in the fracture process. Each indentation

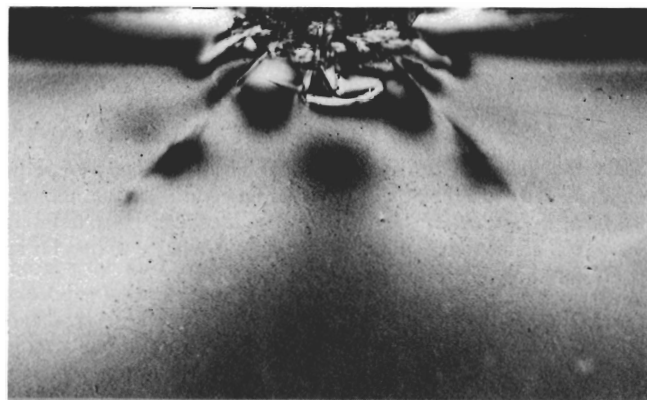


Fig. 3. Profile view of cone-like indentation crack produced by Vickers diamond pyramid in clad material ( $\sigma_R = 0$ ); polarized light,  $P = 50$  N,  $c = 200$   $\mu\text{m}$ .

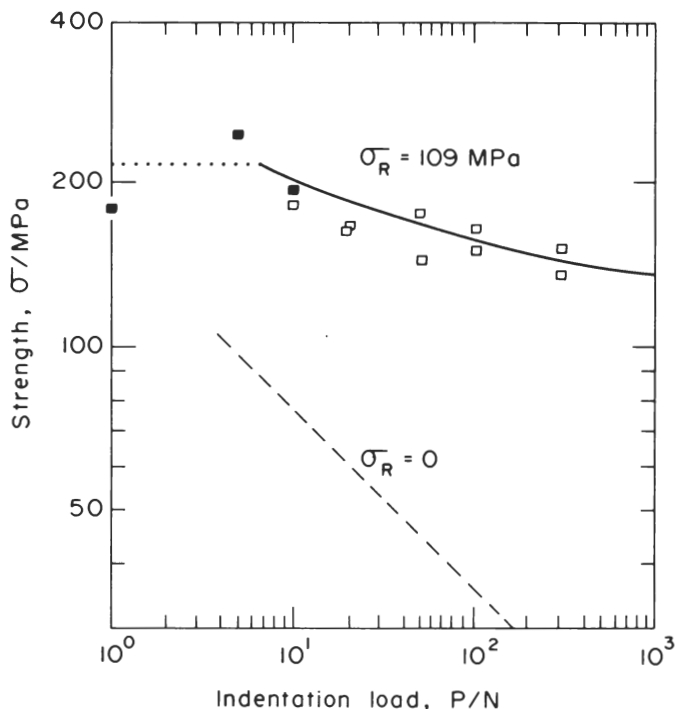


Fig. 4. Strength of air-quenched rods as function of Vickers indentation load, for specimens (including 3 at  $P = 0$ ) in surface compression range  $\sigma_R = (109 \pm 5)$  MPa. Open symbols denote failures from indentation cracks, filled symbols failures from prepresent flaws. Solid line is representation of Eq. (3) for these rods (with horizontal dotted line the strength cutoff averaged over the prepresent-flaw failures), dashed line is equivalent representation for pure clad rods.

cycle was completed in  $\approx 15$  s, and the crosshead speed in the strength test was operated at 0.5 mm/min. The span dimensions in the latter test were set at  $l_i = 40$  mm and  $l_o = 15$  mm.

### III. Results

Specific test runs were made to investigate the effect of severity of contact,  $P$ , and intensity of residual stress,  $\sigma_R$ , on the degradation characteristics of the partially leached rods. The experimental results are shown as the data points in Figs. 4 and 5. A cutoff exists at low load in Fig. 4, indicating a region of behavior in which the indentation cracks are not sufficiently large to dominate preexistent flaws. The loading conditions for the test runs corresponding to the data in Fig. 5 were accordingly chosen to ensure that the starting crack for ultimate failure was indentation-controlled. It is noted that the results for water- and air-quenched specimens are indistinguishable in this figure, so  $P$  and  $\sigma_R$  are the controlling variables in the determination of strength for a given indenter/specimen system. Also included in Fig. 5 are two points for abraded rods; the relative positions of these points on the plot show the abrasion treatment to be considerably less severe than contacts at  $P = 100$  N.

In the interest of establishing a sound basis for optimizing strength design, theoretical evaluations of the functions  $[\sigma(P)]_{\sigma_R}$  and  $[\sigma(\sigma_R)]_P$  were made using an earlier degradation analysis.<sup>10</sup> This analysis combines fracture mechanics relations for the indentation and failure-testing stages into a convenient working expression by eliminating crack size as a variable:

$$\sigma(1 - \sigma_R/\sigma)^{4/3} = A/P^{1/3} \quad (3)$$

For a given system  $A$  is a constant,  $(K_c^4/\chi)^{1/3}/(\pi\Omega_c)^{1/2}$ , where  $K_c$  is the material toughness, and  $\chi$  and  $\Omega_c$  are dimensionless constants, the first relating to indenter/specimen contact conditions and the second to crack geometry (e.g. cone or median geometry). Specific knowledge of the parameters  $K_c$ ,  $\chi$ , and  $\Omega_c$  may be circumvented by suitable calibration of  $A$  if one is concerned with relative rather than absolute strength predictions. Thus in control strength tests on pure

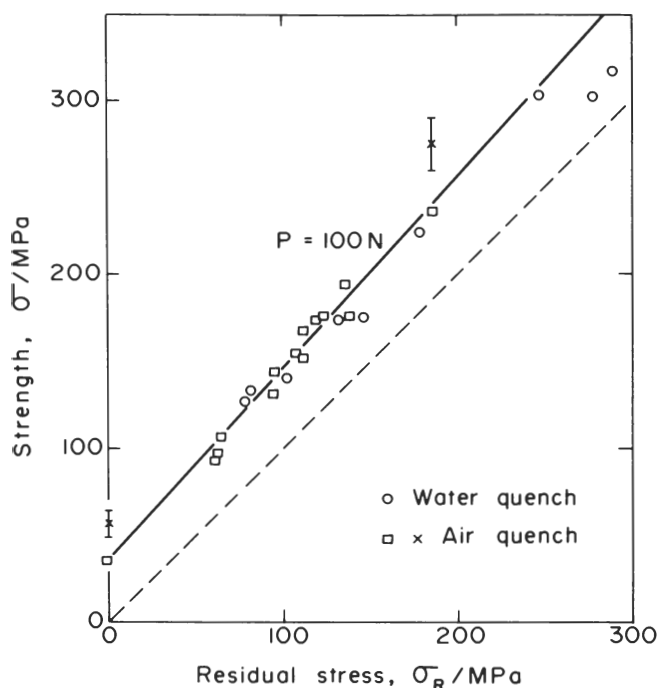


Fig. 5. Strength of water- and air-quenched rods as function of residual compressive stress, for specimens indented at  $P = 100$  N. Solid line is representation of Eq. (3) for these rods, dashed line corresponds to limiting case  $\sigma = \sigma_R$ . Two data points with error bars are for SiC-abraded rods, corresponding to means and standard deviations for  $>20$  specimens each.

clad material ( $a = 0$ ,  $\sigma_R = 0$ , Fig. 2) indented at  $P = 100$  N, a base failure stress  $\sigma = 34.8 \pm 2.0$  MPa (6 rods) was obtained, corresponding to  $A = 162 \pm 9$  MPa  $N^{1/3}$ . The full curves in Figs. 4 and 5 are representations of Eq. (3) based on this value and are seen to agree with the experimental data within the limits of scatter.

#### IV. Discussion

The results of the present study demonstrate the potential usefulness of partially leached glasses in applications where resistance to degradation by particle contact is a paramount consideration. Figure 4 shows that surfaces of moderate residual compression are capable of sustaining high-load contact events without serious loss in strength: according to Eq. (3) the strength should not fall below  $\sigma_R$ . The results of Fig. 5 reinforce this point\* and demonstrate most clearly the strengthening effect of the leaching treatment. A large value of  $\sigma_R$  appears to be a prime requisite in strength design.

However, it should be recalled from Fig. 2 that, for any given set of process variables, an increase in surface compression is gained at the expense of a reduction in clad/core thickness. There is accordingly an increasing danger of the prospective contact crack penetrating the clad, thence causing spontaneous failure of the rod, in the higher-compression specimens. An approximate calculation of the critical loading conditions for such an event to occur is given in Appendix C: although these critical conditions are apparently not closely approached by the data in Figs. 4 and 5, they represent a limit on the strengthening that may ultimately be achieved by a given treatment schedule. In this context, certain avenues may exist in the specimen fabrication for alleviating this restriction: increasing rod radius  $b$  will give, at fixed leaching time (i.e. at constant  $b - a$ ), an increase in ratio  $a/b$ , hence in  $\sigma_R$  (Fig. 2); increasing the quench efficiency, e.g. in going from air to water as quench medium, will again increase  $\sigma_R$  (Fig. 2). In both instances the increase in  $\sigma_R$  obtains without changing clad thickness  $b - a$ , in which case the critical load  $P_c$  in Eq. (C-2) should increase also.

Apart from optimization of process variables, some interesting points arise from the indentation/strength analysis concerning material property requirements. Mention has already been made of the role of differential thermal properties between clad and core in generating large values of residual stress  $\sigma_R$ . Equation (3) suggests that glass compositions should be sought which also maximize the parameter  $A$ . As it turns out, this parameter is relatively insensitive to composition:  $K_c$  is unlikely to vary over a range of much more than 30%<sup>11</sup>;  $\chi$  and  $\Omega_c$  vary by no more than a factor of 2 or 3 as the crack geometry changes from median to cone, i.e. as the glass transforms in mechanical behavior from "normal" (high network modifier content) to "anomalous" (high network former content).<sup>9,12,13</sup> Thus the value  $A = 162$  MPa  $N^{1/3}$  obtained here for the silica-rich clad material (cf.  $A = 84$  MPa  $N^{1/3}$  obtained for soda-lime glass in an earlier study<sup>10</sup>) may be difficult to improve upon to any significant extent. There may nevertheless be some benefit to be gained if the base composition of the glass could be adjusted to give an increase in the elastic modulus of the core material relative to that of the clad: this would lead to a corresponding decrease in  $k$  in Eq. (2), thence to an increase in load-bearing capacity  $Q$  in Eq. (1) for a fixed clad strength.

Our conclusions have been drawn from test results taken under somewhat idealized conditions, namely, static loading of an indenter of regular geometry, equilibrium crack growth, etc. They are, nevertheless, expected to be of general applicability, extending to the important practical problem of impact by particles of arbitrary size and shape.<sup>14,15</sup>

#### APPENDIX A

##### Flexural Stresses in Inhomogeneous, Coaxial Rod

Consider a coaxial rod, core and clad radii  $a$  and  $b$ , respectively, subject to a moment  $M$ , as in the section view of Fig. 1. If  $OXX$  defines the neutral surface, the strain across the section varies linearly with  $y$ , provided the core/clad interface remains coherent. Any difference between the elastic moduli  $E_a$  and  $E_b$  must then give rise to a discontinuity in the stress profile at the clad/core interface. The aim here is to determine the effects of this discontinuity on the tensile stress in the clad surface.

Writing  $\sigma(y) = \sigma_b$  for required stress at  $y = b$ , the strain across the section immediately becomes

$$\epsilon(y) = (\sigma_b/E_b)(y/b) \quad (A-1)$$

The corresponding stress distribution is accordingly given by

$$\begin{aligned} \sigma(y) &= E_a \epsilon(y) = \sigma_b (E_a/E_b)(y/b) & (0 \leq y < a) \\ &= E_b \epsilon(y) = \sigma_b (y/b) & (a < y \leq b) \end{aligned} \quad (A-2)$$

It is convenient now to consider the bending moment  $\sigma(y)y \, dA$  acting over an elemental section area  $dA = (r d\theta) dr$  in the cylindrical coordinate system. Putting  $y = r \sin \theta$  and integrating over the entire section  $A$  then gives the net moment

$$M = (\pi \sigma_b / 4b) [(E_a/E_b - 1)a^4 + b^4] \quad (A-3)$$

For the limiting case of homogeneous rods,  $E_a = E_b$  (or  $a \rightarrow 0$ ), with corresponding stress  $\sigma_b = \sigma_b^0$ , Eq. (A-3) reduces to the familiar result

$$M = (\pi \sigma_b^0 / 4)b^3 \quad (A-4)$$

Since the moments on any section of given geometry must be uniquely determined by the applied loading configuration, the values of  $M$  in Eqs. (A-3) and (A-4) must be identical. Thus, defining  $k = \sigma_b / \sigma_b^0$  as the tensile stress for a clad rod relative to that for an equivalent homogeneous rod, we obtain

$$k = 1 / [1 + (E_a/E_b - 1)(a/b)^4] \quad (A-5)$$

#### APPENDIX B

##### Elastic Moduli of Core and Clad Glass Compositions

Determinations were made of the Young's moduli  $E_a$  and  $E_b$  of pure clad (completely leached) and pure core (unleached) material,

\*Strengths calculated from Eq. (1) on the basis of  $k=1$  actually violate the requirement  $\sigma > \sigma_R$  at large  $\sigma_R$ , emphasizing the necessity to incorporate Eq. (2) as a correction for rod inhomogeneity into the formulation.

respectively. One theoretical and two experimental approaches were adopted.

The first experimental method involved static measurements in flexure. Specimens were stressed in a 3-point bend jig and the deflections of the load points relative to the supports monitored. In conjunction with simple beam theory, knowledge of the load-point displacement and bending load enables an elastic modulus to be evaluated. Allowing for experimental measurement error, values  $E_a = 46.6 \pm 1.4$  and  $E_b = 62.6 \pm 1.5$  GPa were obtained in this way.

In the second experimental method the moduli were measured acoustically. A triple composite resonant system was used, with the specimen rod mounted between two identical quartz transducers: one transducer acts as a generator, the other as a detector, of longitudinal waves.<sup>16</sup> The core and clad specimens were ground to match the transducers in cross-sectional area and their lengths cut to give approximately the same resonant frequency as the transducers. From measurements of the half-wavelength resonant frequency of the composite system, along with the densities ( $\rho_a = 2135 \text{ kg m}^{-3}$  and  $\rho_b = 2180 \text{ kg m}^{-3}$ ) and dimensions of each element, the longitudinal wave velocities for the specimen materials were determined from an appropriate resonance condition.<sup>16</sup> This gave  $E_a = 46.4 \pm 0.4$  GPa and  $E_b = 63.0 \pm 0.5$  GPa.

Finally, an attempt was made to estimate the moduli on theoretical grounds, in terms of the glass compositions. Several workers have developed models for calculating elastic constants along these lines, but a semiempirical approach proposed by Phillips<sup>17</sup> appears to be the most valid for the silicate glass types considered here. His calculation assumes that each component of the glass contributes linearly to Young's modulus in terms of the product of the mole percent concentration and an empirically determined coefficient. For some oxide components this coefficient is constant, for others it depends on the association with network former/modifier sister components. The calculated value for the core composition (62.3%  $\text{SiO}_2$ , 32.3  $\text{B}_2\text{O}_3$ , 1.80  $\text{Na}_2\text{O}$ , 3.57  $\text{K}_2\text{O}$ ) is accordingly  $E_a = 46.6$  GPa, and for the clad composition (93.4%  $\text{SiO}_2$ , 6.5  $\text{B}_2\text{O}_3$ , 0.02  $\text{Na}_2\text{O}$ , 0.10  $\text{K}_2\text{O}$ ) is  $E_b = 68.1$  GPa.

The statically and dynamically determined moduli are seen to agree to within 1% for both core and clad materials. The theoretical evaluation for the core conforms to this level of agreement, but that for the clad shows a discrepancy of  $\approx 8\%$ . Reference to Phillip's paper<sup>17</sup> suggests that the discrepancy may be due to the range of material compositions actually used to calibrate the empirical coefficients mentioned above; whereas the core composition falls within the range used, the clad composition does not. Notwithstanding any such inaccuracies in the theoretical model, the computed moduli confirm the essential difference in elastic properties between the outer and inner regions of the partially leached rods. From these considerations, the values  $E_a = 46.5 \pm 1$  GPa and  $E_b = 63.0 \pm 2$  GPa were adopted, with the uncertainties considered somewhat conservative.

## APPENDIX C

### Critical Loading in Contact-Induced Failure

Consider the growth of a penny-like contact crack (i.e. cone or median), depth  $c$ , through the clad (Fig. 1) as the indentation load is being applied. Under what conditions will this crack become unstable and cause spontaneous rod failure? A complete answer to this question would require a detailed crack integration procedure at all points during the growth,<sup>2</sup> taking into account all the complexities of fracture geometry, modulus change across the core/clad interface, strength of the interface itself, etc. In order to circumvent such complexities it is simply assumed here that the crack will propagate through the clad as if in a homogeneous system, and will reach instability when it penetrates to the core. This criterion does not, of course, relate directly to any specific mode of failure (e.g. repeated bifurcation within the tensile core, separation at the core/clad interface), but nevertheless should provide a reasonable indication of the parameters which control the critical contact loading.

The stress intensity factor for equilibrium contact cracks in a uniform compression field  $\sigma_R$  is<sup>2</sup>

$$K = \chi P/c^{3/2} - \sigma_R(\pi\Omega_c)^{1/2} = K_c \quad (\text{C-1})$$

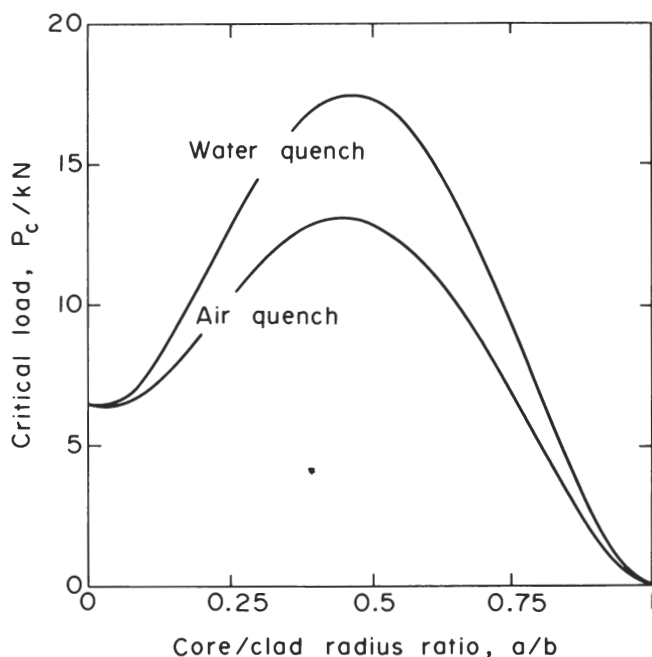


Fig. 1C. Critical contact load for crack penetration through clad as function of core/clad radius ratio.

If failure occurs at  $P = P_c$ ,  $c = b - a$ , this equation gives

$$P_c = (K_c/\chi)(b-a)^{3/2} [1 + \sigma_R(\pi\Omega_c)^{1/2}(b-a)^{1/2}/K_c] \quad (\text{C-2})$$

It is convenient to normalize this expression in terms of the ratio  $a/b$ , recalling (Section II(1)) that  $\sigma_R$  is of the functional form  $\sigma_R(a/b)$ :

$$P_c(a/b) = (K_c b^{3/2}/\chi)(1-a/b)^{3/2} [1 + \sigma_R(a/b)(\pi\Omega_c b)^{1/2} / (1-a/b)^{1/2}/K_c] \quad (\text{C-3})$$

Plots of the function  $P_c(a/b)$  are shown in Fig. 1C for the following values:  $b = 3.5$  mm (average rod radius),  $K_c = 0.72 \text{ MPa m}^{1/2}$  (Vycor\* datum),<sup>11</sup>  $\Omega_c = 0.62$  (cone crack parameter,<sup>12</sup> conjugate to depth  $c$ ),  $\chi = 0.023$  (evaluated from  $A$  (Section III)), with  $\sigma_R(a/b)$  taken from the smooth curves in Fig. 2.

\*Corning Glass Works, Corning, N. Y.

## References

- F. M. Emsberger, "Strength of Brittle Ceramic Materials," *Am. Ceram. Soc. Bull.*, **52** [3] 240-46 (1973).
- B. R. Lawn and D. B. Marshall, "Contact Fracture Resistance of Physically and Chemically Tempered Glass Plates: A Theoretical Model," *Phys. Chem. Glasses*, **18** [1] 7-18 (1977).
- M. G. Drexhage, "Strengthening of Glasses by Phase Separation," Ph. D. Thesis, The Catholic University of America, Washington, D.C., 1977.
- M. G. Drexhage and P. K. Gupta, "Strengthening of Glasses by Partial Leaching"; to be published in the *Journal of the American Ceramic Society*.
- B. R. Lawn and D. B. Marshall, pp. 205-29 in *Fracture Mechanics of Ceramics*, Vol. 3, Edited by R. C. Bradt, D. P. H. Hasselman, and F. F. Lange, Plenum, New York, 1978.
- J. W. Dally and W. F. Riley, *Experimental Stress Analysis*, Ch. 8, McGraw-Hill, New York, 1965.
- D. A. Krohn and A. R. Cooper, "Strengthening of Glass Fibers: I," *J. Am. Ceram. Soc.*, **52** [12] 661-64 (1969).
- B. R. Lawn and T. R. Wilshaw, "Indentation Fracture: Principles and Applications," *J. Mater. Sci.*, **10** [6] 1049-81 (1975).
- A. Arora, D. B. Marshall, B. R. Lawn, and M. V. Swain, "Indentation Deformation/Fracture of Normal and Anomalous Glasses," *J. Non-Cryst. Solids*, **31** [3] 915-28 (1979).
- D. B. Marshall and B. R. Lawn, "Strength Degradation of Thermally Tempered Glass Plates," *J. Am. Ceram. Soc.*, **61** [1-2] 21-27 (1978).
- S. M. Wiederhorn, "Fracture Surface Energy of Glass," *ibid.*, **52** [2] 99-105 (1969).
- B. R. Lawn, S. M. Wiederhorn, and H. H. Johnson, "Strength Degradation of Brittle Surfaces: Blunt Indenters," *ibid.*, **58** [9-10] 428-32 (1975).
- B. R. Lawn, E. R. Fuller, and S. M. Wiederhorn, "Strength Degradation of Brittle Surfaces: Sharp Indenters," *ibid.*, **59** [5-6] 193-97 (1976).
- S. M. Wiederhorn and B. R. Lawn, "Strength Degradation of Glass Impacted with Sharp Particles: I," *ibid.*, **62** [1-2] 66-70 (1979).
- B. R. Lawn, D. B. Marshall, and S. M. Wiederhorn, "Strength Degradation of Glass Impacted with Sharp Particles: II," *ibid.*, pp. 71-74.
- H. F. Pollard, *Sound Waves in Solids*, Ch. 4, Pion, London, 1977.
- C. J. Phillips, "Calculation of Young's Modulus of Elasticity from Composition of Simple and Complex Silicate Glasses," *Glass Technol.*, **5** [6] 216-23 (1964).